

Table 1 Selected bond lengths (Å) and angles (°) for **1a**

Zn(11)–O(11)	1.993(5)	O(13)–C(10)	1.246(10)
Zn(11)–O(101)	1.970(4)	Zn(21)–O(12)	1.965(5)
Zn(11)–O(103)	2.087(5)	Zn(21)–O(201)	2.013(5)
Zn(11)–N(101)	2.057(6)	Zn(21)–O(203)	1.985(5)
Zn(11)–N(103)	2.258(5)	Zn(21)–N(201)	2.027(6)
Zn(12)–O(11)	1.957(5)	Zn(21)–N(203)	2.312(6)
Zn(12)–O(102)	1.984(5)	Zn(22)–O(13)	1.982(5)
Zn(12)–O(103)	2.063(5)	Zn(22)–O(202)	1.998(5)
Zn(12)–N(102)	2.023(6)	Zn(22)–O(203)	1.995(5)
Zn(12)–N(104)	2.307(6)	Zn(22)–N(202)	1.992(7)
O(11)–C(10)	1.321(9)	Zn(22)–N(204)	2.298(5)
O(12)–C(10)	1.259(10)		
O(101)–Zn(11)–N(103)	170.4(2)	O(201)–Zn(21)–N(203)	157.7(2)
O(11)–Zn(11)–N(101)	131.5(2)	O(12)–Zn(21)–N(201)	101.2(2)
O(11)–Zn(11)–O(103)	80.69(19)	O(12)–Zn(21)–O(203)	108.1(2)
N(101)–Zn(11)–O(103)	144.6(2)	N(201)–Zn(21)–O(203)	149.9(2)
O(102)–Zn(12)–N(104)	167.9(2)	O(202)–Zn(22)–N(204)	166.1(2)
O(11)–Zn(12)–N(102)	128.7(2)	O(13)–Zn(22)–N(202)	108.7(2)
O(11)–Zn(12)–O(103)	82.1(2)	O(13)–Zn(22)–O(203)	109.0(2)
N(102)–Zn(12)–O(103)	144.1(2)	N(202)–Zn(22)–O(203)	141.2(2)
Zn(12)–O(103)–Zn(11)	94.4(2)	Zn(21)–O(203)–Zn(22)	107.6(2)
Zn(12)–O(11)–Zn(11)	100.9(2)		

to isolation of $[(Zn_2L)_2(CO_3)] \cdot 4H_2O$, which crystallises as $[(Zn_2L)_2(CO_3)] \cdot 4H_2O \cdot 2CH_3CN$ **1a** and $[(Zn_2L)_2(CO_3)] \cdot 4H_2O$ **1b**. This experiment shows that the H_3L /zinc system can fix carbon dioxide, converting it into the carbonate ligand.

The electrochemical synthesis was performed under a nitrogen stream, in an attempt to avoid air, the most probable source of CO_2 . Concentration of the yellow solution so obtained gives crystals of $[(Zn_2L)_2(CO_3)] \cdot 0.25H_2O \cdot 2CH_3CN$ **1c**. Replacement of nitrogen by an argon stream, in order to avoid or reduce the CO_2 presence to the minimum, does not allow the isolation of any pure product from the reaction cell.

The interaction of zinc and H_3L was also studied by a classical chemical method. Reaction of zinc acetate with H_3L in air yields $[Zn_2L(CH_3COO)] \cdot 2H_2O$. Recrystallisation of the product in acetonitrile/methanol leads to crystals of $[Zn_2L(CH_3COO)] \cdot 2H_2O \cdot CH_3OH$ **2**, which is stable in air in the solid state and in solution. Following a related procedure,¹⁵ $[Zn_2L(CH_3COO)] \cdot 2H_2O$ was reacted with $(CH_3)_4NOH \cdot 5H_2O$ in acetonitrile in air. The insoluble bulk pale yellow material so obtained was characterised by elemental analysis, mass spectrometry and NMR spectroscopy. The signal at *ca.* 165 ppm in the ^{13}C NMR spectrum seems to indicate that the sample is, again, the tetranuclear carbonate-complex. Recrystallisation of the bulk sample in acetonitrile in air gives complex **1a**, corroborated by X-ray diffraction studies.

The fact that the acetate complex could be isolated and was stable in air but yielded the carbonate complex in the presence of $(CH_3)_4NOH \cdot 5H_2O$, seems to indicate that fixation of carbon dioxide only proceeds in a basic medium in this case study. Therefore, it seems that the hydroxy reactant plays an important role in the reaction mechanism of carbon dioxide absorption.

Attempts to corroborate this point were made, since reaction of acetate complexes with hydroxy ligands in an inert atmosphere to yield hydroxy complexes is well documented in the literature.^{13,15,16} Thus, the chemical reaction was carried out in boiled acetonitrile under an argon atmosphere. The pale yellow solid isolated shows a ^{13}C NMR spectrum typical of the tetranuclear carbonate complex. This makes evident that our hard efforts to maintain an inert atmosphere always resulted in adventitious addition of CO_2 to the complex, showing the extraordinary ability of this system to react with carbon dioxide.

X-Ray diffraction studies

Crystal structure of $[(Zn_2L)_2(CO_3)] \cdot 4H_2O \cdot 2CH_3CN$ 1a. Single crystals of $[(Zn_2L)_2(CO_3)] \cdot 4H_2O \cdot 2CH_3CN$ **1a**, $[(Zn_2L)_2(CO_3)] \cdot$

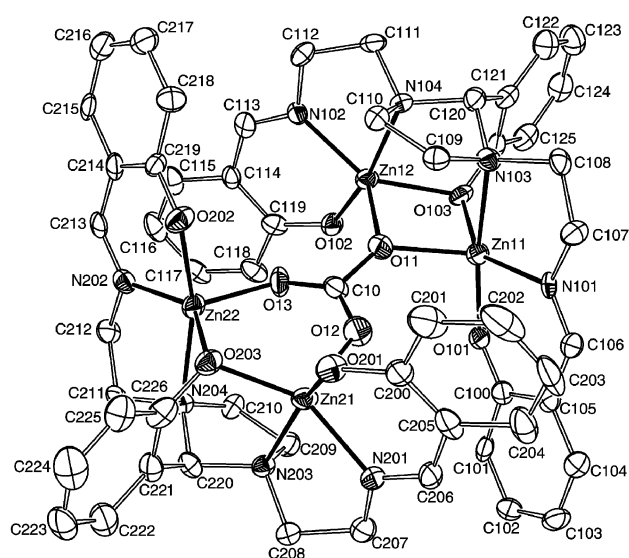


Fig. 1 An ORTEP view of the crystal structure of $[(Zn_2L)_2(CO_3)] \cdot 4H_2O \cdot 2CH_3CN$ **1a**. Solvent molecules are omitted for clarity. Ellipsoids are drawn at 40% probability.

$4H_2O$ **1b** and $[(Zn_2L)_2(CO_3)] \cdot 0.25H_2O \cdot 2CH_3CN$ **1c**, suitable for X-ray diffraction studies, were grown as detailed in the Experimental section. This analysis shows that **1a**, **1b** and **1c** are essentially the same chemical compound and consists of tetranuclear neutral $[(Zn_2L)_2(\mu_4-CO_3)]$ units with acetonitrile and water as solvates. For this reason, only **1a** should be described. The ORTEP diagrams and crystallographic data for **1b** and **1c** are deposited as ESI. †

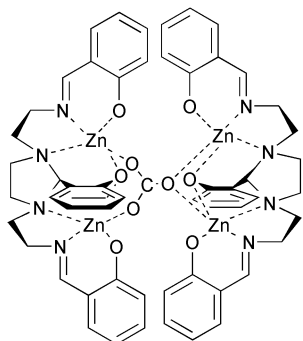
An ORTEP view of **1a** is shown in Fig. 1. Experimental details are given in Table 3 (see Experimental) and selected bond lengths and angles in Table 1.

The structure of the complex can be understood as two dinuclear $[Zn_2L]^+$ units bridged by the carbonate ligand. The compartmental trianionic $[L]^{3-}$ ligand has two tridentate cavities (formed by one phenol oxygen, one imine and one amine nitrogen atom), each one allocating a zinc ion. In addition, the phenol oxygen atom of the middle ligand arm bridges both metal centres. Additionally, a carbonate ligand joins two $[Zn_2L]^+$ units. Thus, the tetranuclear structure can be considered as obtained by assembly of two dinuclear components (Fig. 2).

The four zinc atoms are placed on the vertices of a distorted rectangle (intradinuclear $ZnX1 \cdots ZnX2$ distances of *ca.* 3 Å;

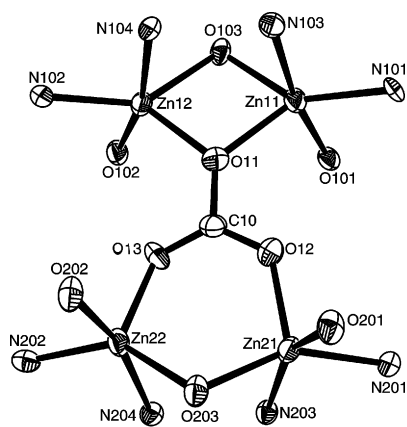
Table 2 Selected bond lengths (Å) and angles (°) for **2**

Zn(11)–O(103)	1.988(3)	Zn(12)–O(103)	1.980(3)
Zn(11)–O(11)	1.990(3)	Zn(12)–O(12)	1.989(3)
Zn(11)–O(101)	1.992(3)	Zn(12)–O(102)	1.997(3)
Zn(11)–N(101)	2.011(3)	Zn(12)–N(102)	2.008(4)
Zn(11)–N(103)	2.414(3)	Zn(12)–N(104)	2.385(3)
O(103)–Zn(11)–O(11)	108.34(13)	O(103)–Zn(12)–O(12)	109.33(13)
O(103)–Zn(11)–N(101)	136.52(12)	O(103)–Zn(12)–N(102)	139.17(14)
O(11)–Zn(11)–N(101)	113.15(14)	O(12)–Zn(12)–N(102)	109.51(15)
O(101)–Zn(11)–N(103)	163.73(14)	O(102)–Zn(12)–N(104)	162.49(13)
Zn(11)–O(103)–Zn(12)	109.32(12)		

**Fig. 2** Schematic representation of the $[\text{Zn}_2\text{L}_2(\text{CO}_3)]$ complex.

interdinuclear $\text{Zn1X} \cdots \text{Zn2X}$ distances of *ca.* 5 Å, with $X = 1, 2$), the shortest $\text{Zn} \cdots \text{Zn}$ distance corresponding to the zinc atoms of the Zn_2O_2 ring (distance $\text{Zn11} \cdots \text{Zn12}$ of 3.0451(13) Å). This distance compares fairly well with those found in dinuclear zinc complexes containing an endogenous and an exogenous O-bridge.¹⁷

Each zinc atom is in a pentacoordinated N_2O_3 environment (Fig. 3). Analysis of the τ parameter [*ca.* 0.4 except for Zn21

**Fig. 3** The core of the tetranuclear complex.

(0.13)] indicates geometry between square pyramidal and trigonal bipyramidal for three of the four zinc atoms and a distorted square pyramidal environment for Zn21 . The $\text{Zn}–\text{N}$ and $\text{Zn}–\text{O}$ distances are in the expected range,^{18–20} with the $\text{Zn}–\text{N}_{\text{imine}}$ distances being significantly shorter than the $\text{Zn}–\text{N}_{\text{amine}}$ ones. The angles around the zinc atoms, which range from 78.4(2) to 170.4(2)°, clearly show the high distortion of the polyhedron.

The carbonate ligand is acting in a $\mu_4-\eta^2-\eta^1-\eta^1$ fashion: one oxygen atom bridges two metal centres, giving rise to a four-membered Zn_2O_2 nearly planar ring, and the other two oxygen atoms are linked in a *syn-syn* binding mode to each one of the remaining zinc atoms and form a six-membered $\text{Zn}_2(\text{O})\text{CO}_2$ chelate ring. The different $\text{Zn}–\text{O}_{\text{carbonate}}$ and $\text{C}–\text{O}_{\text{carbonate}}$ distances reflect the asymmetric nature of the carbonate bridge: the bridging $\mu_2\eta^2-\text{O}$ atom shows the longest

Table 3 Crystal data and structure refinement for **1a** and **2**

	1a	2
Empirical formula	$\text{C}_{59}\text{H}_{68}\text{N}_{10}\text{O}_{13}\text{Zn}_4$	$\text{C}_{30}\text{H}_{37}\text{N}_4\text{O}_8\text{Zn}_2$
Formula weight	1386.71	712.38
Temperature/K	120.0(1)	293(2)
Wavelength/Å	0.71073	0.71073
Crystal system	Monoclinic	Triclinic
Space group	Pn	$P\bar{1}$
<i>a</i> /Å	11.828(2)	10.058(3)
<i>b</i> /Å	17.039(4)	11.470(3)
<i>c</i> /Å	15.706(3)	15.581(4)
α /°	90	94.238(4)
β /°	109.784(4)	93.770(4)
γ /°	90	109.993(4)
<i>Z</i>	2	2
Absorption coefficient/ mm^{-1}	1.664	1.482
Crystal size/ mm^3	$0.24 \times 0.20 \times 0.14$	$0.81 \times 0.28 \times 0.17$
Reflections collected	19198	6822
Independent reflections	9302 [$R(\text{int}) = 0.0328$]	6822
Absorption correction	SADABS	SADABS
Data/restraints/parameters	9302/2/778	6822/0/405
Final <i>R</i> indices	$R1 = 0.0499$	$R1 = 0.0468$
[$I > 2\sigma(I)$]	$wR2 = 0.1184$	$wR2 = 0.1482$
<i>R</i> indices (all data)	$R1 = 0.0668$	$R1 = 0.0659$
	$wR2 = 0.1320$	$wR2 = 0.1631$

$\text{C}–\text{O}$ distance, as expected.^{13,21–23} Besides, the $\text{Zn}–\mu_2\eta^2-\text{O}_{\text{carbonate}}$ distances are significantly different for the same $[\text{Zn}_2\text{L}]^+$ unit, showing the asymmetry of the $\text{Zn}–\text{O}_{\text{carbonate}}-\text{Zn}$ bridge. This also occurs with the $\text{Zn}–\mu_2-\text{O}_{\text{phenol}}$ distances, that clearly shows the non-symmetric nature of the $\text{Zn}–\text{O}_{\text{phenol}}-\text{Zn}$ bridge.

Complex **1a** contains four water molecules in the unit cell that give rise to intramolecular hydrogen bonds. For each $[\text{Zn}_2\text{L}]^+$ unit, one water molecule interacts with both phenol oxygen atoms [distances $\text{O}(1\text{W}) \cdots \text{O}(101)$, $\text{O}(1\text{W}) \cdots \text{O}(102)$, $\text{O}(3\text{W}) \cdots \text{O}(201)$ and $\text{O}(3\text{W}) \cdots \text{O}(202)$ ranging from 2.750(8) to 2.878(8) Å]. The second water molecule per dinuclear unit is hydrogen bonded to the first one [distances $\text{O}(1\text{W}) \cdots \text{O}(2\text{W})$ 2.719(9) Å and $\text{O}(3\text{W}) \cdots \text{O}(4\text{W})$ 2.725(9) Å]. These interactions contribute to ensure the cohesion of the crystal lattice, which is highly ordered.

Crystal structure of $[\text{Zn}_2\text{L}(\text{CH}_3\text{COO})] \cdot 2\text{H}_2\text{O} \cdot \text{CH}_3\text{OH}$ **2.** An ORTEP view of **2** is shown in Fig. 4. Experimental details are given in Table 3 and selected bond lengths and angles in Table 2.

Complex **2** consists of dinuclear neutral $\text{Zn}_2\text{L}(\text{CH}_3\text{COO})$ units with methanol and water as solvates. Each zinc atom is in an N_2O_3 environment, made up of one amine nitrogen, one imine nitrogen and one terminal phenol oxygen atom. Besides, the metal atoms are doubly bridged by an endogenous phenol oxygen atom of the central ligand arm and by an exogenous acetate group, acting as bridging bidentate in a *syn-syn* mode. The coordination geometry can be considered as intermediate between square pyramidal and trigonal bipyramidal, as it is

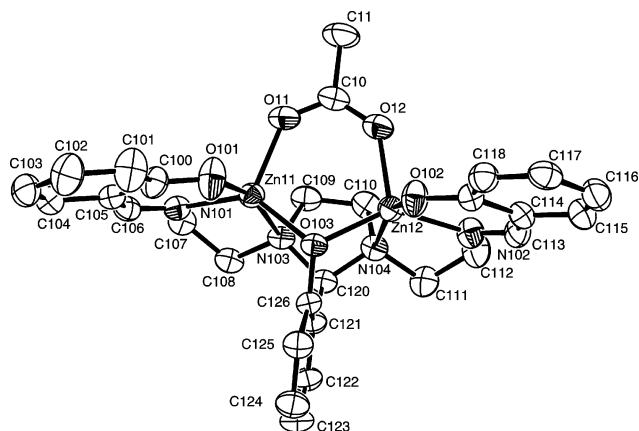


Fig. 4 An ORTEP view of $[\text{Zn}_2\text{L}(\text{CH}_3\text{COO})]\cdot 2\text{H}_2\text{O}\cdot \text{CH}_3\text{OH}$ **2**. Solvent molecules are omitted for clarity. Ellipsoids are drawn at 40% of probability.

reflected by the index of trigonality τ (*ca.* 0.45 for Zn11 and 0.4 for Zn12).

The Zn–N and Zn–O distances are in the expected range.^{13,17,18} The Zn–O distances for the bridging phenoxy interactions indicate that this bridge is practically symmetric [Zn(11)–O(103) 1.988(3) Å; Zn(12)–O(103) 1.980(3) Å]. Similarly, the Zn(11)–O(11) and Zn(12)–O(12) distances [Zn(11)–O(11) 1.990(3) Å; Zn(12)–O(12) 1.989(3) Å] show a high degree of symmetry for the acetate bridge. The intermetallic separation is *ca.* 3.24 Å and compares fairly well with metal distances found for similar complexes.^{15,24}

The angles around zinc atoms, ranging from 78.85(13) to 163.73(14) show a high distortion from the ideal geometry.

Complex **2** shows an intricate hydrogen bond scheme among solvate molecules and the phenol and acetate oxygen atoms. Two water molecules [O(2w) and O(3w)] are at 50% occupancy, with O(3w) disordered over two sites. Thus, one water molecule (O1w) gives rise to intramolecular interactions with both terminal phenol oxygen atoms [O(1W) \cdots O(101) 2.935(5) Å; O(1W) \cdots O(102) 2.827(5) Å] and with the methanol molecule [O(1S) \cdots O(1W) 2.746(8) Å]. The methanol solvent also interacts with O(3w) [O(1S) \cdots O(3W) 2.734(18) Å]. O(2w) shows a short intramolecular interaction with an acetate oxygen atom [O(2W) \cdots O(12) 2.932(9) Å] and two long intermolecular hydrogen bonds with one terminal phenol and one acetate oxygen atom of a neighbouring unit [O(2W) \cdots O(101)* 3.210(10) Å; O(2W) \cdots O(11)* 3.269(11) Å]. In addition, a water molecule of a neighbouring unit [O(2W*)] interacts with O(101) and O(11). This give rise to a disposition of the molecules in the unit cell as shown in Fig. 5, that resembles a tetranuclear dimer made up of two weakly joined dinuclear monomers.

Spectral characterisation

The IR, mass, ¹H and ¹³C NMR spectra of $[(\text{Zn}_2\text{L})_2(\text{CO}_3)]\cdot 4\text{H}_2\text{O}$ and $[\text{Zn}_2\text{L}(\text{CH}_3\text{COO})]\cdot 2\text{H}_2\text{O}$ (see Experimental section) are consistent with their expected structures and with stability of the complexes in solution.^{25–28}

The ¹H NMR spectra of both complexes show two sets of aromatic signals, arising from the non-equivalent terminal and central ligand arms. This result also states that there is only one species and that both $[\text{Zn}_2\text{L}]^+$ units of the carbonate complex are equivalent in solution. A singlet at 1.99 ppm (3 H) for $[\text{Zn}_2\text{L}(\text{CH}_3\text{COO})]\cdot 2\text{H}_2\text{O}$ agrees with the coordination of the acetate group to the metal centres in solution.

In addition, the ¹³C NMR spectrum of $[\text{Zn}_2\text{L}(\text{CH}_3\text{COO})]\cdot 2\text{H}_2\text{O}$ shows peaks typical of coordinated acetate (163.27 and 23.55 ppm). The spectrum of the carbonate complex shows a new peak at 165.11 ppm, assigned to the carbonate group. This

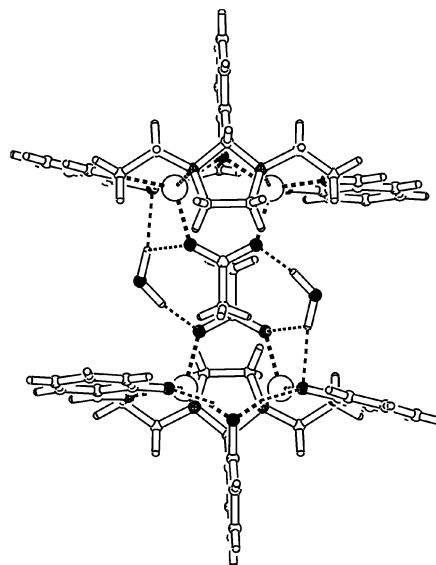


Fig. 5 A view of the disposition of two neighbouring molecules in complex **2**, showing the weakly joined dinuclear units.

signal is in the range of those found for carbonate-bridged complexes.^{12,29–31}

Finally, it should be noted that both ¹³C and ¹H NMR spectra of the complex obtained by chemical reaction between $[\text{Zn}_2\text{L}(\text{CH}_3\text{COO})]\cdot 2\text{H}_2\text{O}$ and $(\text{CH}_3)_4\text{NOH}\cdot 5\text{H}_2\text{O}$, clearly indicates that the acetate ligand was replaced by a carbonate ligand.

As a result of the studies performed and the characterisation techniques employed, it can be concluded that the zinc/ H_3L system in an electrochemical cell readily absorbs carbon dioxide to generate a tetranuclear zinc carbonate compound in a unique step. The chemical reaction of zinc acetate with H_3L in air allows isolation of $[\text{Zn}_2\text{L}(\text{CH}_3\text{COO})]\cdot 2\text{H}_2\text{O}$, that can not survive in solution in the presence of $(\text{CH}_3)_4\text{NOH}$, yielding, again, the carbonate complex. Attempts to maintain an inert atmosphere always resulted in addition of CO_2 to the complex, preventing the isolation of any intermediate and evidencing the extremely high reactivity of this system towards carbon dioxide.

Experimental

Chemicals

All solvents, salicylaldehyde, triethylenetetramine, tetramethylammonium hydroxide pentahydrate and zinc acetate dihydrate are commercially available and were used without further purification. Zinc (Ega Chemie) was used as *ca.* 2 × 2 cm² plates.

Physical measurements

Elemental analyses of C, H and N were performed on a Carlo Erba EA 1108 analyser. NMR spectra were recorded on a Bruker AC-300 spectrometer using DMSO-*d*₆ as solvent. Infrared spectra were recorded as KBr pellets on a Bio-Rad FTS 135 spectrophotometer in the range 4000–600 cm⁻¹. Electrospray mass spectra were obtained on a Hewlett-Packard LC/MS spectrometer, in methanol as solvent.

Synthesis of the ligand and metal complexes

H_3L was prepared following a related procedure¹⁴ and fully characterised by elemental analysis, mass spectrometry, IR and ¹H NMR spectroscopy. Anal. Calc. for H_3L (C₂₇H₃₀N₄O₃): C, 70.7; H, 6.5; N, 12.2. Found: C, 70.2; H, 6.7; N, 12.4%. MS(ES): *m/z* 459 (H_4L^+). IR (KBr, ν/cm^{-1}): 1632 (C=N), 3434 (OH). ¹H NMR (300 MHz, DMSO-*d*₆): 2.64 (q, 2H, H^{2ax}), 2.70 (q, 2H, H^{1ax}), 2.84 (q, H^{2eq}), 3.35 (m, H^{1eq}), 3.60 (t, 4H, H³), 4.02

(s, 1H, H¹⁷), 6.65 (d, 1H, H¹⁴), 6.73 (dd, 1H, H¹²), 6.89–6.83 (m, 4H, H⁷ + H⁹), 7.15 (m, 2H, H¹¹ + H¹³), 7.31 (dd, 2H, H⁸), 7.36 (d, 2H, H⁶), 8.43 (s, 2H, H⁴), 10.86 (br, 1H, OH), 13.77 (br, 2H, OH).

[(Zn₂L)₂(CO₃)]·4H₂O: an acetonitrile solution of H₃L (0.1 g, 0.218 mmol), containing *ca.* 10 mg of tetramethylammonium perchlorate, was electrolysed at 10 mA, for 2 h 20 min, using a platinum wire as cathode and a zinc plate as anode. Slow evaporation of the resultant yellow solution yielded crystals of [(Zn₂L)₂(CO₃)]·4H₂O·2CH₃CN **1a** and [(Zn₂L)₂(CO₃)]·4H₂O **1b**, suitable for X-ray diffraction studies. The analysis of the bulk sample is in agreement with the [(Zn₂L)₂(CO₃)]·4H₂O proposed stoichiometry. Calc. for [(Zn₂L)₂(CO₃)]·4H₂O (C₅₅H₆₂N₈O₁₃Zn₄): C, 50.6; H, 4.8; N, 8.6. Found: C, 50.5; H, 4.7; N, 8.7%. MS(ES): *m/z* 585 [Zn₂L]⁺, 629 [Zn₂L(CO₃)]⁺, 647 [Zn₂L(CO₃)₂H]⁺, 1217 [(Zn₂L)₂(CO₃)]⁺, 1231 [(Zn₂L)₂(CO₃)H]⁺. IR (KBr, *v*/cm⁻¹): 1535, 1347 (CO₃), 1633 (C=N), 3434 (OH). NMR (300 MHz, DMSO-*d*₆): ¹H NMR: 2.71–2.56 (m, 6H, H^{1ax} + H^{2ax} + 2H³), 3.23 (m, 2H, H^{2eq}), 3.63 (t, 2H, 2H³), 3.83 (m, 2H, H^{1eq}), 3.99 (s, 1H, H¹⁷), 6.41 (dd, 2H, H⁷), 6.56–6.66 (m, 4H, 2H⁹ + H¹² + H¹⁴), 7.02–7.10 (m, 4H, 2H⁶ + H¹¹ + H¹³), 7.19 (dd, 2H, H⁸), 8.31 (s, 2H, H⁴). ¹³C NMR: 49.96 (C²), 52.34 (C³), 53.86 (C¹), 89.88 (C¹⁷), 117.96, 116.50 (C⁵ + C¹⁶), 130.76 (C¹⁰), 135.35, 133.65, 132.21, 122.31, 122.05, 121.26, 112.32 (C⁶–C⁹ + C¹¹–C¹⁴), 165.11 (CO₃), 170.84 (C⁴), 171.24 (C¹⁵).

The same complex was obtained when an acetonitrile solution of Zn₂L(CH₃COO)·2H₂O was treated with tetramethylammonium hydroxide pentahydrate in air and/or under an argon (99.999%) stream.

[(Zn₂L)₂(CO₃)]·0.25H₂O·2CH₃CN **1c**: through an acetonitrile (80 mL) solution of H₃L (0.1 g, 0.218 mmol), containing *ca.* 10 mg of tetramethylammonium perchlorate, a nitrogen stream was passed for 1 h. Then, the solution was electrolysed under a nitrogen stream at 10 mA, for 2 h 20 min, using a platinum wire as cathode and a zinc plate as anode. The resultant yellow solution was concentrated and after reduction of its volume to ½, small yellow crystals of **1c**, suitable for X-ray diffraction studies, were isolated.

[Zn₂L(CH₃COO)]·2H₂O: To a methanol (20 mL) solution of Zn(CH₃COO)·2H₂O (0.25 g, 1.14 mmol), an acetonitrile (20 mL) solution of H₃L (0.26 g, 0.57 mmol) was added. The resultant yellow solution was stirred in air for 4 h, and a pale yellow solid precipitated. The solid was filtered and washed with diethylether. Recrystallisation in methanol/acetonitrile yields crystals of [Zn₂L(CH₃COO)]·2H₂O·CH₃OH **2**, suitable for X-ray diffraction studies. Calc. for Zn₂L(CH₃COO)·2H₂O (C₂₉H₃₃N₄O₅Zn₂): C, 51.1; H, 5.0; N, 8.2. Found: C, 50.7; H, 5.0; N, 8.0%. MS(ES): *m/z* 585 [Zn₂L]⁺, 645 [Zn₂L(CH₃COOH)]⁺. IR (KBr, *v*/cm⁻¹): 1574, 1450 (COO), 1630 (C=N), 3447 (OH). NMR (300 MHz, DMSO-*d*₆): ¹H NMR: 1.99 (s, 3H, CH₃), 2.62 (m, 2H, 2H^{3ax}), 2.72–2.80 (m, 4H, H^{1ax} + H^{2ax}), 3.36 (m, 2H, H^{2eq}), 3.62 (m, 2H, 2H^{1eq}), 3.75 (m, 2H, 2H^{3eq}), 4.12 (s, 1H, H¹⁷), 6.40 (dd, 2H, H⁷), 6.72–6.79 (m, 6H, 2H⁸ + 2H⁹ + H¹² + H¹⁴), 7.04–7.18 (m, 4H, 2H⁶ + H¹¹ + H¹³), 8.32 (s, 2H, H⁴). ¹³C NMR: 23.55 (CH₃), 50.25 (C²), 53.97 (C³), 54.29 (C¹), 89.51 (C¹⁷), 117.59, 118.92 (C⁵ + C¹⁶), 131.03 (C¹⁰), 132.36, 133.83, 135.24, 123.52, 122.18, 121.47, 112.38 (C⁶–C⁹ + C¹¹–C¹⁴), 163.27 (COO), 171.01 (C⁴), 171.66 (C¹⁵).

Crystallographic measurements

Crystal data and details of refinement are given in Table 3.

[(Zn₂L)₂(CO₃)]·4H₂O·2CH₃CN **1a** and [Zn₂L(CH₃COO)]·2H₂O·CH₃OH **2**. Crystals of **1a** and **2**, suitable for single-crystal X-ray studies, were obtained as previously described. Data were collected at 120 K for **1a** and 293 K for **2** on a

Bruker SMART 1000 diffractometer, employing graphite-monochromated Mo-Kα ($\lambda = 0.71073$ Å) radiation. The structures were solved by direct methods and refined by full matrix least squares based on F^2 .³² An SADABS absorption correction was applied. Non-hydrogen atoms were anisotropically refined. Hydrogen atoms bonded to carbon were included in the structure factor calculation in idealised positions but not refined. Hydrogen attached to oxygen atoms were located in the Fourier map or not included.

CCDC reference numbers 189066 and 178741.

See <http://www.rsc.org/suppdata/dt/b2/b209328f/> for crystallographic data in CIF or other electronic format.

References

- 1 A. Behr, *Carbon dioxide activation by metal complexes*, VCH, New York, 1988.
- 2 D. J. Darensbourg and M. Holtcamp, *Coord. Chem. Rev.*, 1996, **152**, 155.
- 3 W. Leitner, *Coord. Chem. Rev.*, 1996, **153**, 257.
- 4 D. H. Gibson, *Chem. Rev.*, 1996, **96**, 2063.
- 5 X. Yin and J. R. Moss, *Coord. Chem. Rev.*, 1999, **181**, 27.
- 6 D. Walter, M. R. Ruben and S. Rau, *Coord. Chem. Rev.*, 1999, **182**, 67.
- 7 R. H. Bode, W. L. Driessen, F. B. Hulsberg, J. Reedijk and A. L. Spek, *Eur. J. Inorg. Chem.*, 1999, 505.
- 8 M. Kunert, M. Bräuer, O. Klobes, H. Görls, E. Dinjus and E. Anders, *Eur. J. Inorg. Chem.*, 2000, 1803.
- 9 M. Minato, D.-Y. Zhou, K.-I. Sumiura, R. Hirabayashi, Y. Yamaguchi and T. Ito, *Chem. Commun.*, 2001, 2654.
- 10 I. Bertini, *Struct. Bonding (Berlin)*, 1982, **48**, 45.
- 11 E. Kimura, *Acc. Chem. Res.*, 2001, **34**, 171 and references therein.
- 12 H. Adams, D. Bradshaw and D. E. Fenton, *J. Chem. Soc., Dalton Trans.*, 2001, 3407.
- 13 M. Döring, M. Ciesielski, O. Walter and H. Görls, *Eur. J. Inorg. Chem.*, 2002, 1615.
- 14 L.-W. Yang, S. Liu, E. Wong, S.J. Rettig and C. Orvig, *Inorg. Chem.*, 1995, **34**, 2164.
- 15 R. A. Allred, A. M. Arif and L. M. Berreau, *J. Chem. Soc., Dalton Trans.*, 2002, 300.
- 16 C. Fernandes, A. Neves, A. J. Bortoluzzi, B. Szpoganicz and E. Schwingel, *Inorg. Chem. Commun.*, 2001, **4**, 354.
- 17 (a) H. Adams, D. Bradshaw and D. E. Fenton, *Eur. J. Inorg. Chem.*, 2002, 535; (b) H. Adams, D. Bradshaw and D. E. Fenton, *Inorg. Chem. Commun.*, 2002, **5**, 12.
- 18 A. Sousa, M. R. Bermejo, M. Fondo, A. García-Deibe, A. Sousa-Pedrares and O. Piro, *New J. Chem.*, 2001, **25**, 647.
- 19 N. A. Bailey, E. D. McKenzie and J. M. Worthington, *Inorg. Chim. Acta*, 1977, **25**, L137.
- 20 U. Mukhopadhyay, L. Govindasamy, K. Ravikumar, D. Velmurugan and D. Ray, *Inorg. Chem. Commun.*, 1998, **1**, 152.
- 21 F. W. B. Einstein and A. C. Willis, *Inorg. Chem.*, 1981, **20**, 609.
- 22 A. Escuer, E. Peñalba, R. Vicente, X. Solans and M. J. Font-Badía, *J. Chem. Soc., Dalton Trans.*, 1997, 2315.
- 23 D. Armentano, G. De Munno, F. Lloret and M. Julve, *Inorg. Chem.*, 1999, **38**, 3744.
- 24 H. Adams, D. Bradshaw and D. E. Fenton, *J. Chem. Soc., Dalton Trans.*, 2002, 925.
- 25 G. B. Deacon and R. J. Phillips, *Coord. Chem. Rev.*, 1980, **23**, 227.
- 26 A. L. van der Brenk, K. A. Byriel, D. P. Fairlie, L. R. Gahan, G. R. Hanson, C. J. Hawkins, A. Jones, C. H. L. Kennard, B. Moubaraki and K. S. Murray, *Inorg. Chem.*, 1994, **33**, 3549.
- 27 U. N. Andersen, C. J. McKenzie and G. Bojosen, *Inorg. Chem.*, 1995, **34**, 1435.
- 28 D. F. Evans and D. A. Jakubovic, *J. Chem. Soc., Dalton Trans.*, 1988, 2927.
- 29 N. Kitajima, S. Hikichi, M. Tanaka and Y. Moro-oka, *J. Am. Chem. Soc.*, 1993, **115**, 5496.
- 30 (a) A. Schrodt, A. Neubrand and R. van Eldick, *Inorg. Chem.*, 1997, **36**, 4579; (b) Z.-W. Mao, F. W. Heinemann, G. Liehr and R. van Eldick, *J. Chem. Soc., Dalton Trans.*, 2001, 3652.
- 31 M. J. Manos, A. D. Keremidas, J. D. Woollins, A. M. Z. Slawin and T. A. Kabanos, *J. Chem. Soc., Dalton Trans.*, 2001, 3419.
- 32 G. M. Sheldrick, SHELX97 Programs for Crystal Structure Analysis, Institut für Anorganische Chemie der Universität, Göttingen, Germany, 1998.